

Wind loads on industrial solar panel arrays and supporting roof structure

Graeme S. Wood[†]

Department of Civil Engineering, University of Sydney, NSW 2006, Australia

Roy O. Denoon[‡]

Ove Arup and Partners, Level 5 Festival Walk, Kowloon Tong, Hong Kong

Kenny C.S. Kwok^{‡†}

Department of Civil Engineering, University of Sydney, NSW 2006, Australia

Abstract. Wind tunnel pressure tests were conducted on a 1:100 scale model of a large industrial building with solar panels mounted parallel to the flat roof. The model form was chosen to have the same aspect ratio as the Texas Tech University test building. Pressures were simultaneously measured on the roof, and on the topside and underside of the solar panel, the latter two combining to produce a nett panel pressure. For the configurations tested, varying both the lateral spacing between the panels and the height of the panels above the roof surface had little influence on the measured pressures, except at the leading edge. The orientation of the panels with respect to the wind flow and the proximity of the panels to the leading edge had a greater effect on the measured pressure distributions. The pressure coefficients are compared against the results for the roof with no panels attached. The model results with no panels attached agreed well with full-scale results from the Texas Tech test building.

Key words: solar panels; wind loading; wind tunnel testing; pressure measurements.

1. Introduction

The use of solar panel technology has recently increased dramatically in both domestic and industrial applications. This increased usage has been driven by the increasing financial cost of power, and the public desire to produce a greater proportion of energy from renewable resources. The initial capital cost of solar technology is generally greater than traditional sources of energy. However, the running costs are minimal and if production is sufficient, the user may sell energy back to the supplier.

Domestic solar panel systems are generally small and mounted flush or raised slightly, typically around 100mm, above the roof cladding. They will therefore be subjected to topside pressures

[†] Lecturer

[‡] Consulting Wind Engineer

^{‡†} Professor



Fig. 1 Typical application of raised solar panels on a large roof

similar to those acting on the roof cladding system without the solar panels attached, thereby the structural wind loading will not change significantly. To meet the energy requirements of an industrial building, large areas of the roof must be covered with solar panels. To allow for ventilation of the panels, to reduce overheating of the elements, and to facilitate maintenance, the solar panels on industrial buildings are generally raised up to 1m above the roof cladding. For maximum efficiency, solar panels should be angled to the sun, although it is often considered simpler and more architecturally pleasing for the panels to be mounted parallel to the roof. A typical example of a solar panel layout on a large building is shown in Fig. 1. The effect of the solar panel position on the wind loading of the roof cladding and the solar panel support structure is the purpose of this research.

There have been few studies carried out on the wind loading of buildings with solar panels mounted on the roof. Chevalien and Norton (1979) placed angled rows of solar panels on a model building in a wind tunnel and determined that the first row of collectors provided sheltering for the successive rows of panels. As underlined by Lee (1982), the boundary layer profile, or the supporting building were not adequately modelled. Tieleman *et al.* (1980) studied the effect of solar panels mounted on predominantly domestic buildings, but also investigated arrays of panels mounted upon a flat roofed generic industrial building. These panels were mounted at 45° and 60°, and the effects of sheltering from the first row of panels were discussed. Unfortunately, they were not able to measure simultaneous pressures on both sides of the panel. Radu *et al.* (1986) mounted inclined solar panels on the flat roof of a five-storey residential building and measured mean pressures on both sides of the panels through an internal manifold system. There were no details of the frequency response of the manifold system. Significant shielding effects from the building and the first row of solar panels were reported. Radu and Axinte (1989) investigated the effect of architectural attic features on the wind loading on a vertical panel mounted on the roof of a five-storey building. It was found that the larger the height of the attic, the smaller the mean nett pressure acting on the solar panel.

The determination of peak nett design pressures for the design of solar panels and their supporting structures, and the effects of the solar panel on the roof cladding have been investigated in this study for a generic flat-roofed industrial building.

2. Modelling the building and the natural wind

The generic 1:100 scale model building is shown in Fig. 2, and dimensions are detailed in Fig. 3.



Fig. 2 1:100 scale model with solar panels attached

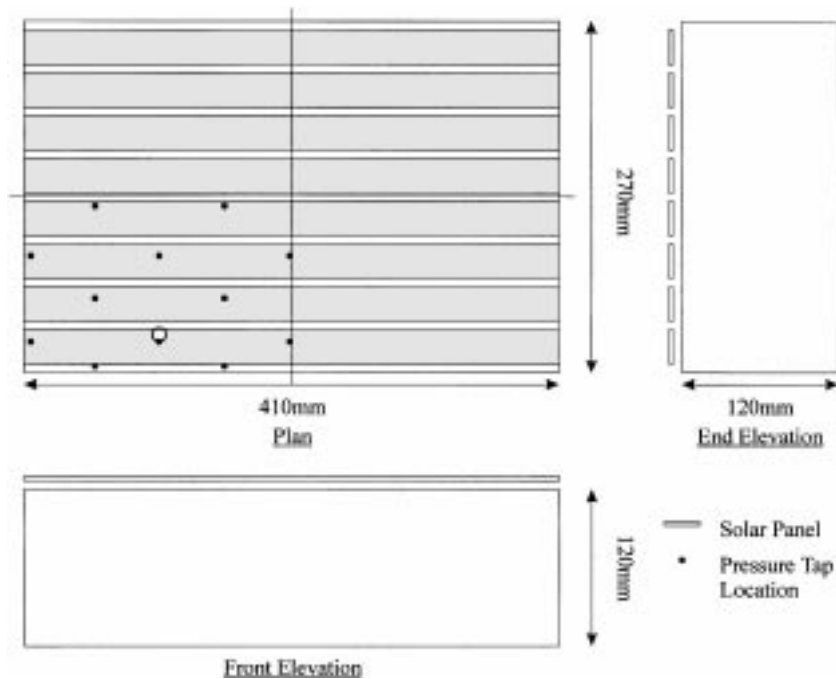


Fig. 3 Plan and elevations of the test model

The solar panels represent typical installations on large roofs, being 27 mm wide (2.7 m full-scale) and running the entire length of the structure. The panels were constructed from 3 mm thick acrylic, threaded through steel rods for support, to minimise blockage, and for ease of changing the panel layout configuration. The model was tested with the panels mounted at three different heights above the roof cladding, 6 mm, 10 mm and 14 mm, and at three different lateral spacings, 4 mm, 6 mm and 8 mm gaps between the panels. Fig. 3 shows the layout for the panels raised 10 mm above the roof and with a spacing of 6 mm between the panels. When spaced at 8 mm, the panels lay flush with the front edge of the roof.

As the building was rectangular in plan, there was no surround model, and the solar panels were

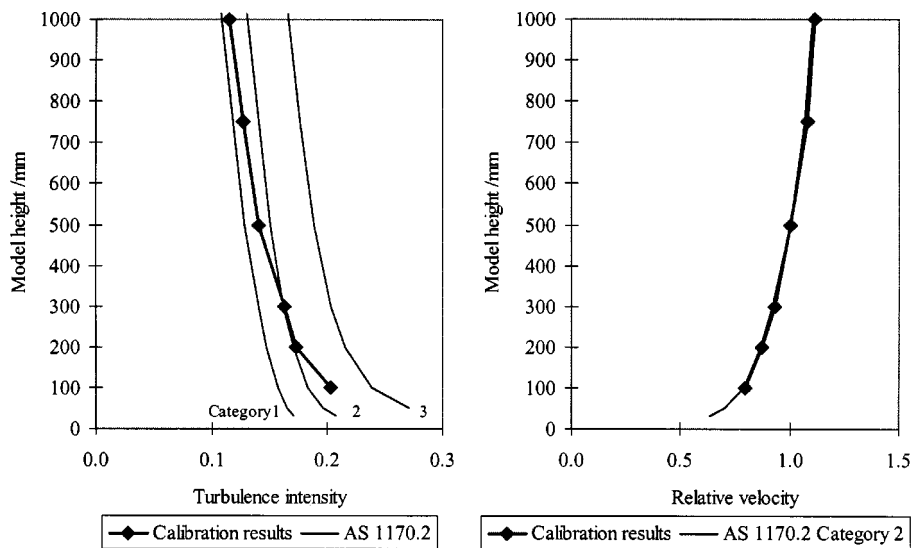


Fig. 4 1:100 scale model velocity and turbulence intensity profiles

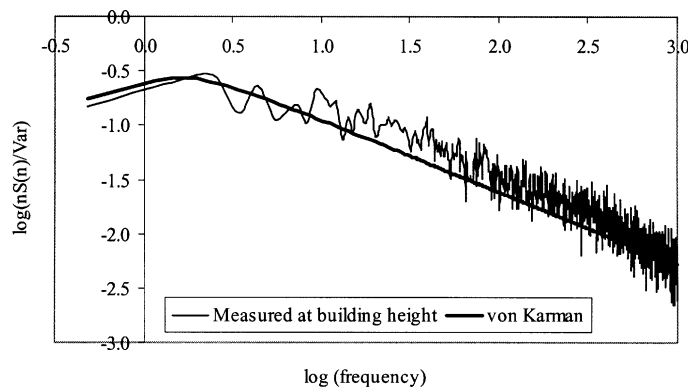


Fig. 5 Power spectral density at model building height

always mounted centrally on the roof, only a quarter of the roof was pressure tapped. At each pressure tap location on the solar panels, shown as dots in Fig. 3, there were three pressure tappings: one each on the panel topside, panel underside, and the roof.

The approaching wind was modelled in the wind tunnel by air flow passing over a fetch of floor-mounted roughness elements preceded by a vorticity generating fence and spires spanning the width of the tunnel. The approach wind velocity profile and wind turbulence characteristics were consistent with a 1:100 scale model of a category 2 boundary layer profile as defined in AS1170.2-1989, (Standards Australia 1989) as shown in Fig. 4. The longitudinal power spectral density at building height is compared with the von Karman (1948) spectrum in Fig. 5.

3. Pressure measurement system

The pressure measurement system was of a closed form. The 32 pressure taps on the model were

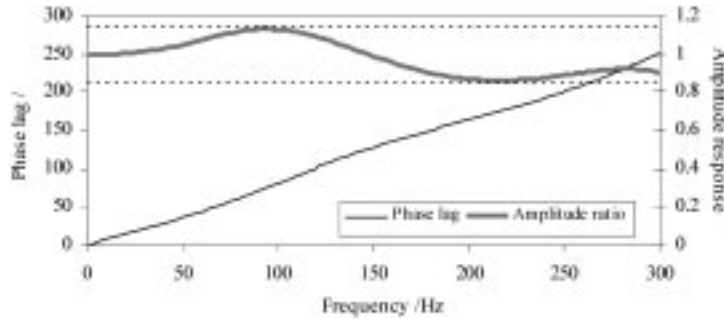


Fig. 6 Phase and amplitude response of the tubing system

connected to Honeywell Type 163 pressure transducers via a short length of vinyl tubing containing two restrictors to reduce resonant effects. The amplitude and phase responses of the system were measured using the calibration equipment described by Holmes and Lewis (1987). The amplitude response was flat, to within 15%, up to 300 Hz, and the phase response was close to linear over this range, Fig. 6.

The model length scale used in the test was 1:100 and the velocity scale was approximately 1:3 (for a 50 year return period wind speed). This gave a model to full-scale time scale of about 1:33. Thus, the model pressure measurement system having a frequency response up to 300 Hz could respond accurately to pressure fluctuations up to prototype values of about 9 Hz. The solar panels were not considered to react to such high frequency, hence the signal was low pass filtered at 100 Hz, representing a full-scale frequency of 3 Hz.

4. Testing programme

Simultaneous wind pressures were measured at the 32 pressure taps around the model for wind directions normal to the faces of the building. The model was tested with solar panels at three different heights above the roof, and at three lateral spacings, as well as the benchmark test with no panels attached. Although only a quarter of the roof was pressure tapped, the symmetry of the experiment allowed the pressure distribution for the entire roof to be evaluated. The pressures were measured relative to the wind tunnel static pressure which was obtained from the static tapping of a Pitot-static tube mounted upstream of the model at a height of 1 m. The mean dynamic wind pressure of the approaching wind flow was also measured using the Pitot-static tube and used as the reference dynamic pressure. These pressures were used to determine a pressure coefficient referenced to the mean dynamic pressure at a height of 1 m as per Eq. (1). The velocity ratio between the reference height and the roof height was measured using a pair of single hot wire anemometers. This allowed the pressure coefficient to be expressed with respect to mean wind speed at eaves height, Eq. (2).

$$C_{p,ref} = \frac{p - p_s}{p_T - p_s} \quad (1)$$

$$C_{p,bldg} = C_{p,ref} \left(\frac{\bar{V}_{ref}}{\bar{V}_{bldg}} \right)^2 \quad (2)$$

where : $C_{p,z}$ pressure coefficient with respect to mean wind speed at model height z
 p pressure measured on the model
 p_s mean static pressure measured at reference height
 p_T mean total pressure measured at reference height
 \bar{V}_z mean velocity measured at height z

The mean and standard deviation pressure coefficients were calculated directly from the time series. The maximum and minimum pressure coefficients were determined from the distribution of peaks, using an upcrossing analysis, Rofail and Kwok (1992).

The pressure signal output from the pressure transducer was amplified, low-pass filtered at 100 Hz, digitised, and stored on a micro-computer, on which all the analysis was carried out. A sampling time of 110 seconds was used, which corresponded to a duration of approximately one hour at prototype scale.

5. Results

5.1. Comparison with full-scale data

The model was first tested without the solar panels attached in order for the results to be compared with full-scale data from the Texas Tech University test building. The Texas Tech building is located on the outskirts of Lubbock, in the Texas plains and has dimensions $9.1 \text{ m} \times 13.7 \text{ m} \times 4.0 \text{ m}$ high. The terrain category surrounding the building corresponds to terrain category 2 in AS1170.2-1989 (Standards Australia 1989). Pressure series for this test building in various orientations were obtained from the Texas Tech Internet site. Fig. 7 shows the comparison between the full-scale and model buildings for the wind normal to the long face of the building. The full-scale test record used for the analysis was M15N541. As can be seen from Fig. 7, both the measured mean and peak pressure coefficients referenced to building height are similar for both the model and full-scale buildings.

5.2. Comparison with Australian wind loading code AS1170.2-1989

The results of the test with no panels attached was compared with the Australian wind loading

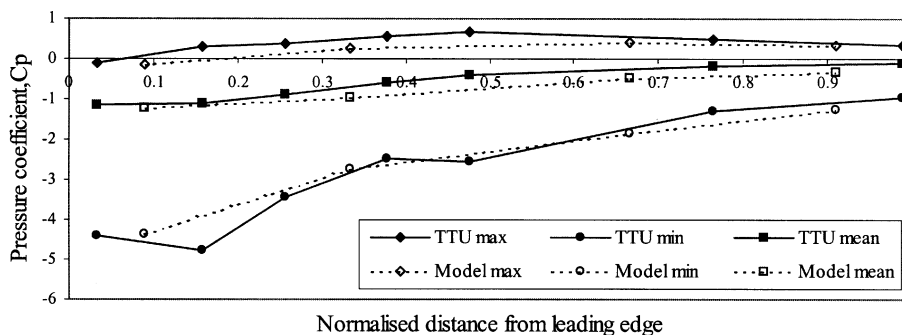


Fig. 7 Comparison with full-scale data

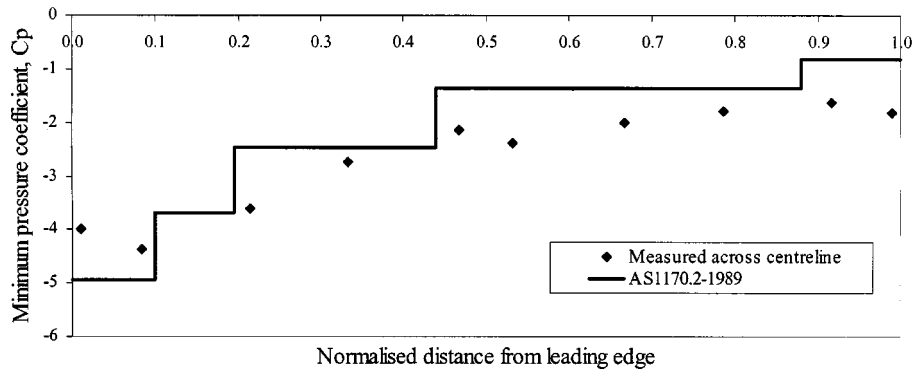


Fig. 8 Comparison with AS1170.2-1989 (Standards Australia 1989)

code, AS1170.2-1989, (Standards Australia 1989). It can be seen from Fig. 8, for wind normal to the long face of the building, that AS1170.2-1989 underestimates the pressure coefficients remote from the leading edge of the building. This is considered to be caused by the higher model turbulence intensity than in the code.

5.3. Influence of solar panels

With the solar panels in position on the roof, the pressures measured on the underside of the solar panel should be similar to those on the roof. Fig. 9 shows a portion of a typical pressure record for the three taps at the location circled on Fig. 3, with the panels at a prototype height of 1 m and a lateral panel spacing of 600 mm. It is evident from Fig. 9 that the roof topside and the panel underside have almost identical pressure histories. The nett panel pressure is calculated by subtracting the panel underside pressure from the panel topside pressure for each record in the time sample. Thus, negative nett pressures act upwards and positive nett pressures act downwards. Peak nett pressures are required for the design of the solar panel and the immediate support system and will be transferred to the roof as a series of point or line loads depending on the structural support system employed. The total load transferred to the structure will therefore be a combination of the distributed load on the roof cladding and the point or line load transferred from the solar panel

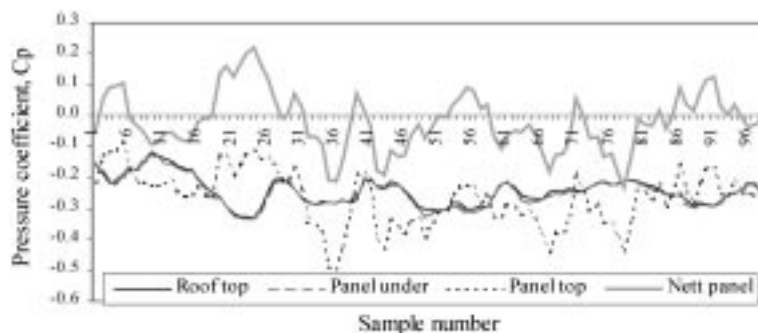


Fig. 9 Typical sample of pressure record for three taps at a single location circled in Fig. 3

support structure. An indication of any change in the magnitude of the total load transferred to the supporting structure, due to the addition of solar panels, can be estimated by comparing the panel topside pressure with the roof pressure measured without the solar panels, as the roof topside and panel underside are approximately equal and opposite.

Upcrossing and spectral analyses were carried out on all signals to determine if the presence of the panels caused a change in the distribution of the peaks or to identify any natural frequencies in the system. Both analyses indicated that there were no significant differences between the measurements with and without the panels attached, except for the roof tappings near the leading edge. At these locations the signal became less intermittent when the panels were attached, which would indicate that the edge panels were tending to stabilise the flow.

5.4. The effect of height on the wind loads

The results reported in this section were all carried out with a prototype lateral spacing between the panels of 600mm, but the trends were similar for the other panel spacings tested.

Figs. 10 and 11 show the effect on the measured peak pressure coefficients of changing the height of the solar panel above the roof. For design purposes, these are compared with the results for the

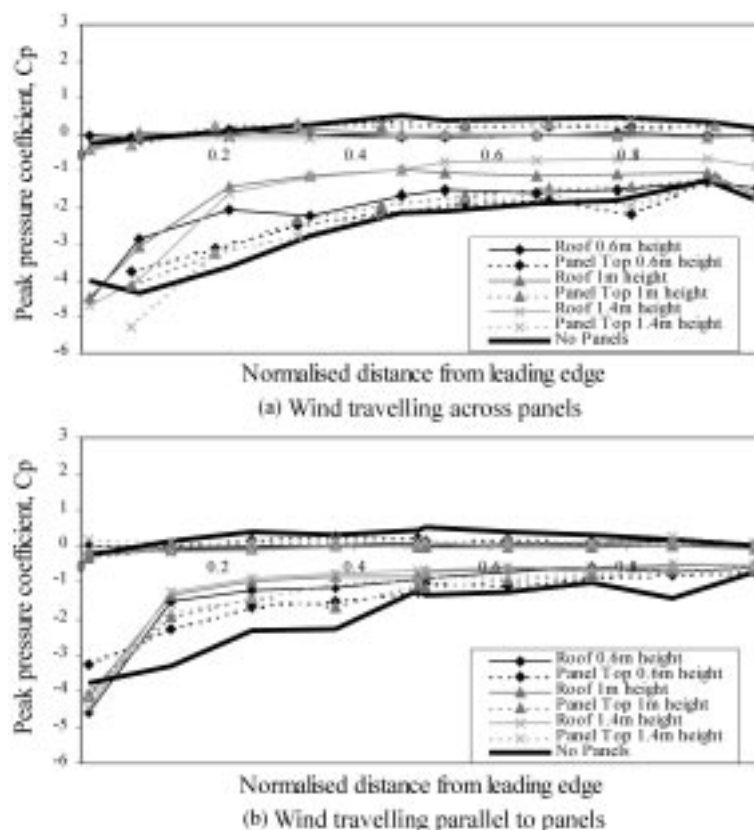


Fig. 10 Effect of panel height above the roof on roof and panel topside pressure coefficients along the centrelines of the building

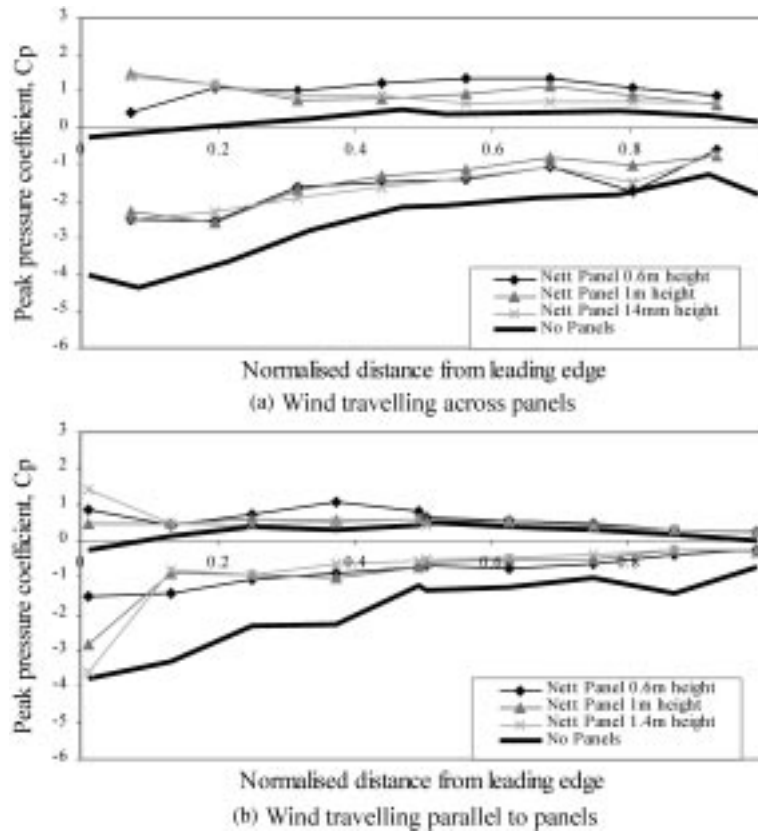


Fig. 11 Effect of panel height above the roof on nett panel pressure coefficients along the centrelines of the building

roof without solar panels.

5.5. Panel topside pressure coefficients

Changing the height of the solar panels above the roof has little influence on the measured panel topside peak negative pressure coefficients over the range of heights tested, except at the leading edge, Fig. 10. Close to the leading edge, the panel topside peak negative pressure coefficients increase in magnitude as the panel height above the roof increases. The peak positive pressure coefficients are not significantly affected by the change in offset height.

The panel topside peak negative pressure coefficients are generally slightly smaller in magnitude than for the roof without solar panels, except at the leading edge, Fig. 10. This indicates that the roof uplift design load would generally decrease with the addition of solar panels, particularly for the wind parallel to the panels. However, for all wind directions tested at the leading edge, the peak negative pressure coefficients for the larger panel heights are greater in magnitude than for the roof without solar panels, Fig. 10. The variability of the peak negative pressure coefficients at the leading edge is greater when the wind is travelling across the panels, Fig. 10a, compared with when the wind is parallel to the solar panels, Fig. 10b.

Close to the leading edge, the increase in panel topside pressure coefficients for the larger panel heights, compared to the roof pressure coefficients without solar panels indicates that the structural roof load will increase. The structural loading will change from a purely distributed load, to a combination of a distributed load and a point or line loading, depending on the support system employed.

The panel topside peak positive pressure coefficients are generally lower than for the roof without panels attached and are of a very small magnitude. This will result in the total roof downward load decreasing with the addition of solar panels.

5.6. Roof cladding pressure coefficients

The peak negative pressure coefficients for the roof with solar panels are generally smaller in magnitude than for the roof without solar panels, except at the leading edge, Fig. 10. At the leading edge, these pressures are greater, by up to 15%, than those measured on the roof with no panels attached. This indicates that the cladding loads at the leading edge are increased due to the presence of the solar panels. Remote from the leading edge, the roof surface is partially shielded by the panels from the outer fluctuating flow.

The rate of increase in the magnitude of peak negative roof pressure coefficients, with distance from the leading edge is similar regardless of the wind direction. Remote from the leading edge the peak negative roof pressures tend to increase with a decrease in offset height, particularly for wind travelling across the panels.

The peak positive pressure coefficients are generally lower than those measured on the roof with no solar panels attached and are of a small magnitude.

5.7. Nett panel pressure coefficients

The peak nett negative pressures, Fig. 11, are all significantly lower in magnitude than the results for the roof without the panels. However, the peak nett positive pressure coefficients tend to be greater in magnitude than the no panel configuration for the entire length of the panel. Fig. 12 shows a comparison between the peak measured nett pressure coefficient, independent of panel configuration, and design pressure coefficients calculated from the Australian wind loading code (Standards Australia 1989) assuming the roof can be designed as a flat and monoslope free roof. From Fig. 12 it can be seen that the current wind loading code is conservative for the uplift loading on the support structure, but will be unconservative for the downward loads when the wind is travelling across the panels. These sections of the Australian wind loading code are not truly applicable to this situation: the flat roof case does not take into account the flow under the panels; and the monoslope free roof does not account of venting between the panels.

5.8. The effect of lateral panel spacing on the wind loads

The results presented in this section were all obtained with the solar panels mounted at a prototype height above the roof of 1 m, but the trends were similar for the other heights tested.

Figs. 13 and 14 show the effects on the measured peak pressure coefficients of changing the lateral spacing between the solar panels. For design purposes, these are compared against the results for the roof without solar panels.

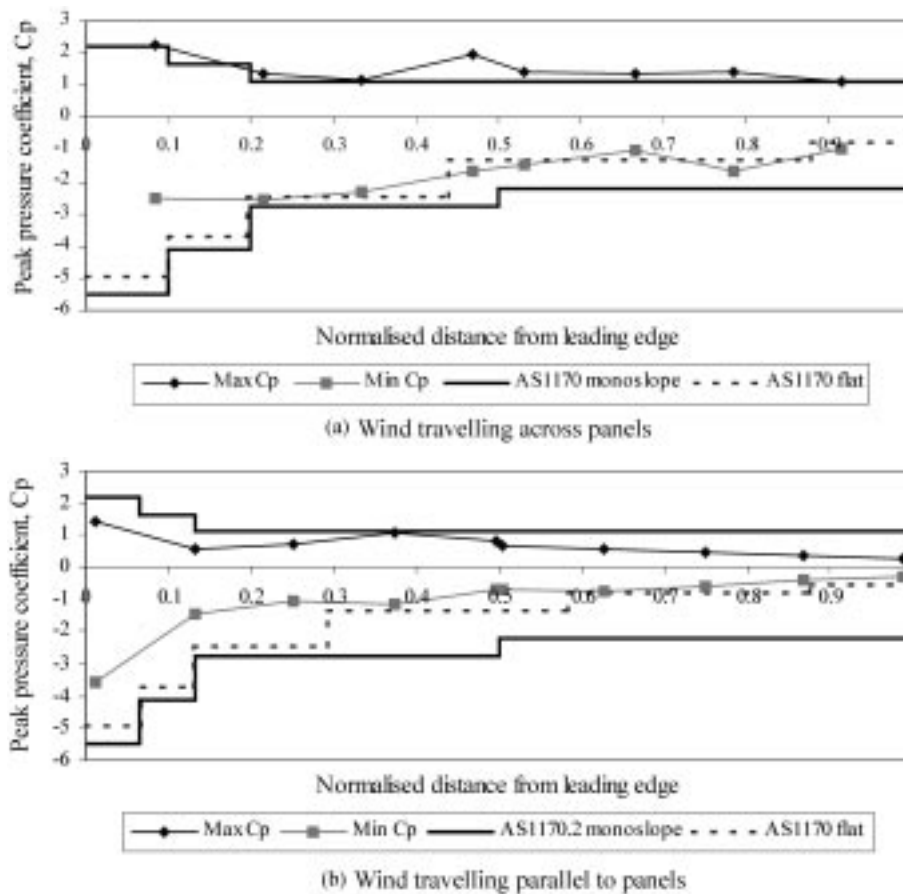


Fig. 12 Comparison between peak measured peak pressure coefficients and AS1170.2-1989 (Standards Australia 1989) for a monoslope and flat roof

5.9. Panel topside pressure coefficients

Fig. 13 shows that near the leading edge the peak pressure coefficients measured on the panel topside do not change significantly with lateral panel spacing, and are similar to the roof without solar panels.

Generally, both the panel topside positive and negative peak pressure coefficients, Fig. 13, are lower in magnitude than those measured on the roof without the panels. This would indicate that the total roof load would decrease compared to that without panels. This loading will change from a distributed load to a combination of a distributed load and a point or line loading depending on the support system employed.

5.10. Roof cladding pressure coefficients

The roof cladding peak negative pressure coefficients, Fig. 13, are generally lower in magnitude than those measured for the roof without the panels attached, except at the leading edge. The

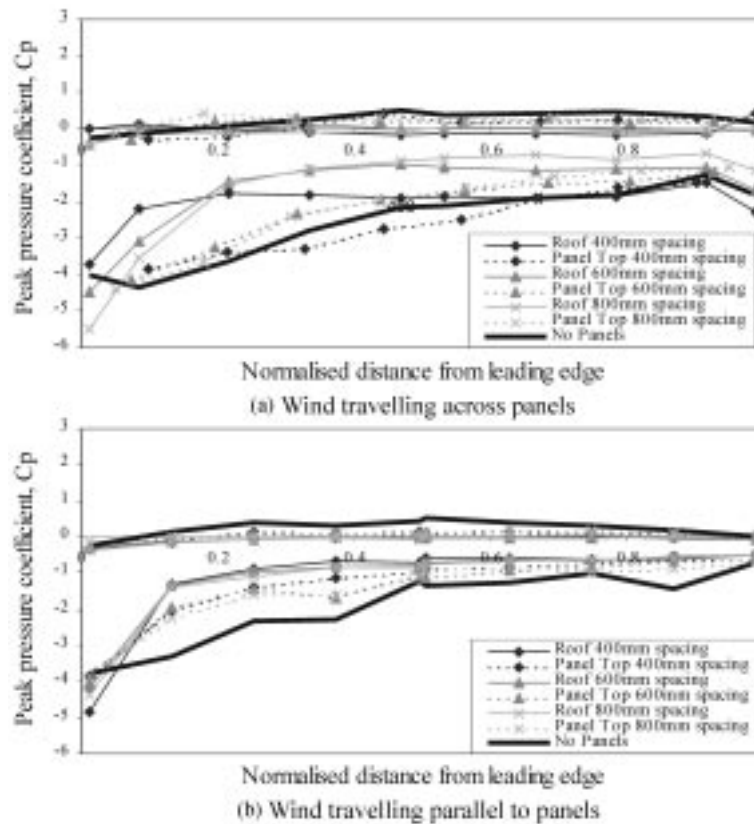


Fig. 13 Effect of panel lateral spacing on roof and panel topside pressure coefficients along the centrelines of the building

greatest increase occurs near the leading edge when the panels are situated flush with the leading edge and perpendicular to the wind flow.

Fig. 13a shows for wind travelling across the solar panels that the magnitude of the peak negative pressure coefficients on the roof increase at the leading edge, as the spacing between the panels increases, but the opposite is true at locations remote from the leading edge. This is primarily caused by the fact that the solar panels were not always mounted flush with the leading edge of the building: as the spacing between the panels decreased, the setback from the leading edge increased. When the prototype lateral panel spacing was 800 mm, the panels were flush with the building edge. This causes the panel position to change relative to the separated region, dramatically altering the flow pattern around the panel. When the flow is parallel to the solar panels, Fig. 13b, the smaller the spacing between the panels the higher the peak negative pressure coefficient at the leading edge, due to a decrease in the venting between panels.

Fig. 13 shows that the peak positive pressure coefficients are not significantly altered by the panel orientation or lateral spacing. Their magnitudes are generally small and lower than those for the roof without solar panels.

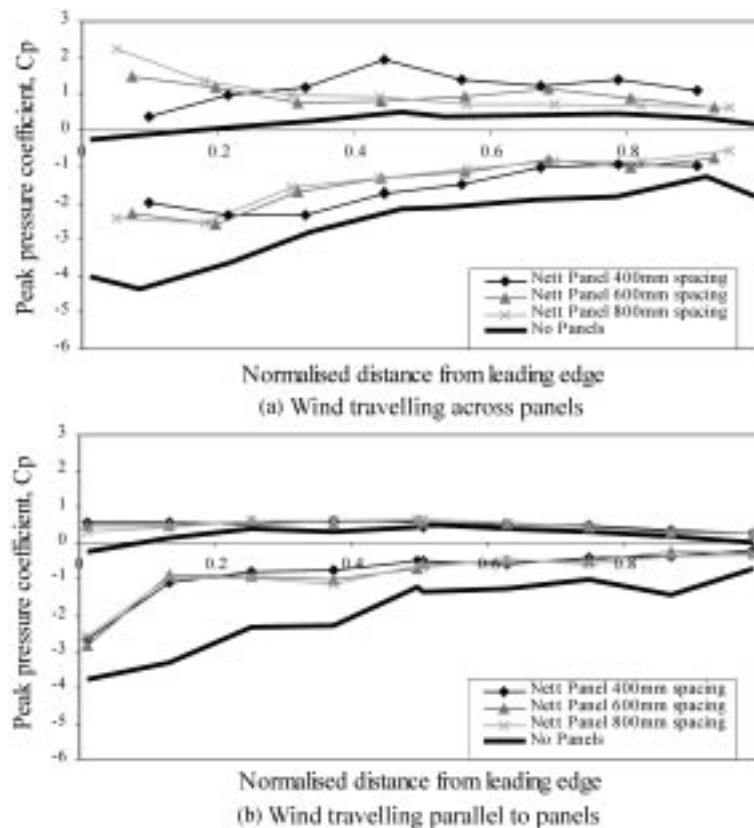


Fig. 14 Effect of panel lateral spacing on nett panel pressure coefficients along the centrelines of the building

5.11. Nett panel pressure coefficients

The peak nett negative panel pressures, Fig. 14, are all significantly lower in magnitude than the corresponding results for the roof with no panels attached, but the peak positive pressure coefficients are all greater. This is again considered to be due to the flow under the panels causing a downward acting force on the panel underside. These significant downward pressures should be incorporated into the design of the support structure, and will be transmitted into the local roof structure.

6. Conclusions

Wind tunnel pressure tests were conducted on a generic industrial building with and without solar panels mounted on the roof. A parametric study was undertaken to investigate the effect of the height of the panels above the roof and the lateral spacing between the panels on the pressures measured on the roof and the solar panels.

The measured mean and peak pressure coefficients agree well with those measured on the full-scale Texas Tech University test building.

Within the range tested, the height of the panels above the roof and the lateral spacing between the panels was shown to have little influence on the measured panel topside and nett pressure

coefficients, except at the leading edge. The orientation of the panels with respect to the wind direction and the proximity of the panel to the leading edge were shown to have a more marked effect.

Any change in the total wind load acting on the roof structure can be evaluated by comparing the panel topside pressure coefficient with that for the roof without the solar panels attached. With the solar panels attached the total wind load on the roof increases at the leading edge, but reduces rapidly behind the leading edge. The structural load changes from a distributed load to a combination of a distributed load and a point or line loading depending on the panel support system employed.

The roof cladding load increases at the leading edge with the solar panels attached, but decreases rapidly behind the leading edge, particularly for the cases with larger panel height and closer proximity to the roof leading edge.

The nett pressure coefficient gives the peak design pressure for the solar panel and the immediate support structure. The peak negative nett panel pressure coefficients are significantly lower than those measured for a roof with no solar panels attached, due to the flow beneath the panel. However, the peak positive nett pressure coefficients are significantly greater in magnitude than those for a roof with no solar panels attached.

Acknowledgements

The authors acknowledge the experimental work carried out by Mr. Ben Eddy and Ms. Sonia Worrall as part of their final year undergraduate honours thesis at The University of Sydney. The authors also acknowledge the advice of Dr. Richard Watkins and the technical assistance of Mr. Mark McLean.

References

- Chevalien, L. and Norton, J. (1979), "Wind loads on solar collector panels and support structure", Aerospace Engineering Department, Texas A&M University.
- Holmes, J.D. and Lewis, R.E. (1987), "Optimisation of dynamic pressure measuring system", *J. Wind Eng. Ind. Aerod.*, **25**(3), 249-290.
- Lee, B., (1982), "A review of data on wind loads on solar collectors", Department of Building Science, University of Sheffield, BS 70.
- Radu, A., Axinte, E. and Theohari, C. (1986), "Steady wind pressures on solar collectors on flat-roofed buildings", *J. Wind Eng. Ind. Aerod.*, **23**, 249-258.
- Radu, A. and Axinte, E. (1989), "Wind forces on structures supporting solar collectors", *J. Wind Eng. Ind. Aerod.*, **32**, 93-100.
- Rofail, A.W. and Kwok, K.C.S. (1992), "A reliability study of wind tunnel results for cladding pressure", *J. Wind Eng. Ind. Aerod.*, **41-44**, 2413-2424.
- Standards Australia (1989), Australian Standard, SAA Loading Code, Part 2: Wind Loads, AS1170.2-1989, Standards Australia.
- Tieleman, H.W., Akins, E. and Sparks, R. (1980), "An investigation of wind loads on solar collectors", Virginia State University, VPI-E-80-1, Blacksburg, VA.
- Von Karman, T. (1948), "Progress in the statistical theory of turbulence", *Proc. Nat. Academy of Sciences*, **34**, 530-539.